Supporting Information

Synthesis and photocatalytic activity of BiOBr nanosheets with tunable crystal facets and sizes

Yuwei Mi,[a] Haiping Li,[b] Yongfang Zhang,[a] Na Du,[a] Wanguo Hou*[a, b]

[a] *Key Laboratory of Colloid and Interface Chemistry (Ministry of Education), Shandong University, Jinan 250100, P.R. China.*

[b] *National Engineering Research Center for Colloidal Materials, Shandong University, Jinan 250100, P.R. China.*

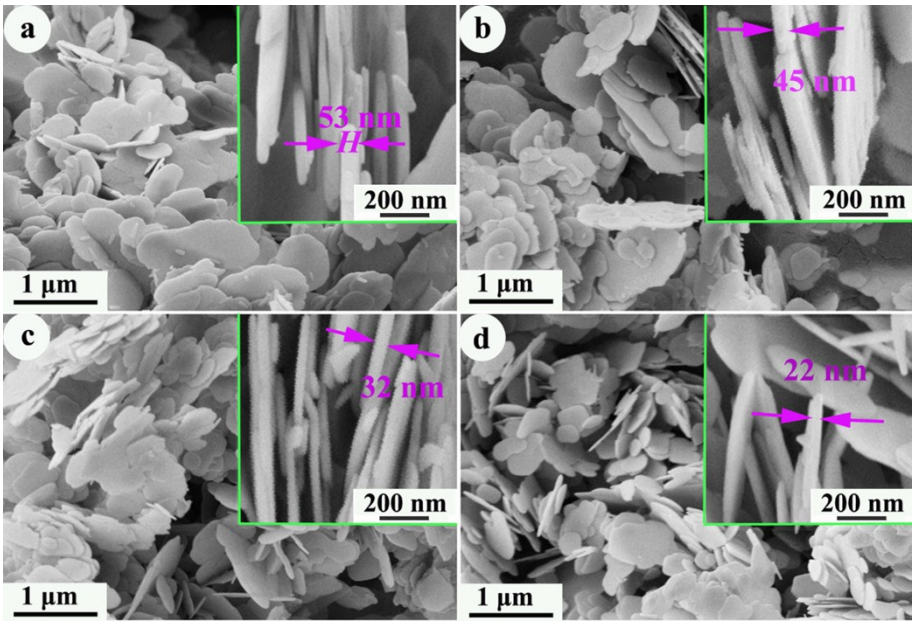

Fig. S1. SEM images of the BiOBr samples: (a) P7.5, (b) P12.5, (c) P22.5, and (d) P27.5. Insets indicate nanosheet thickness of samples.

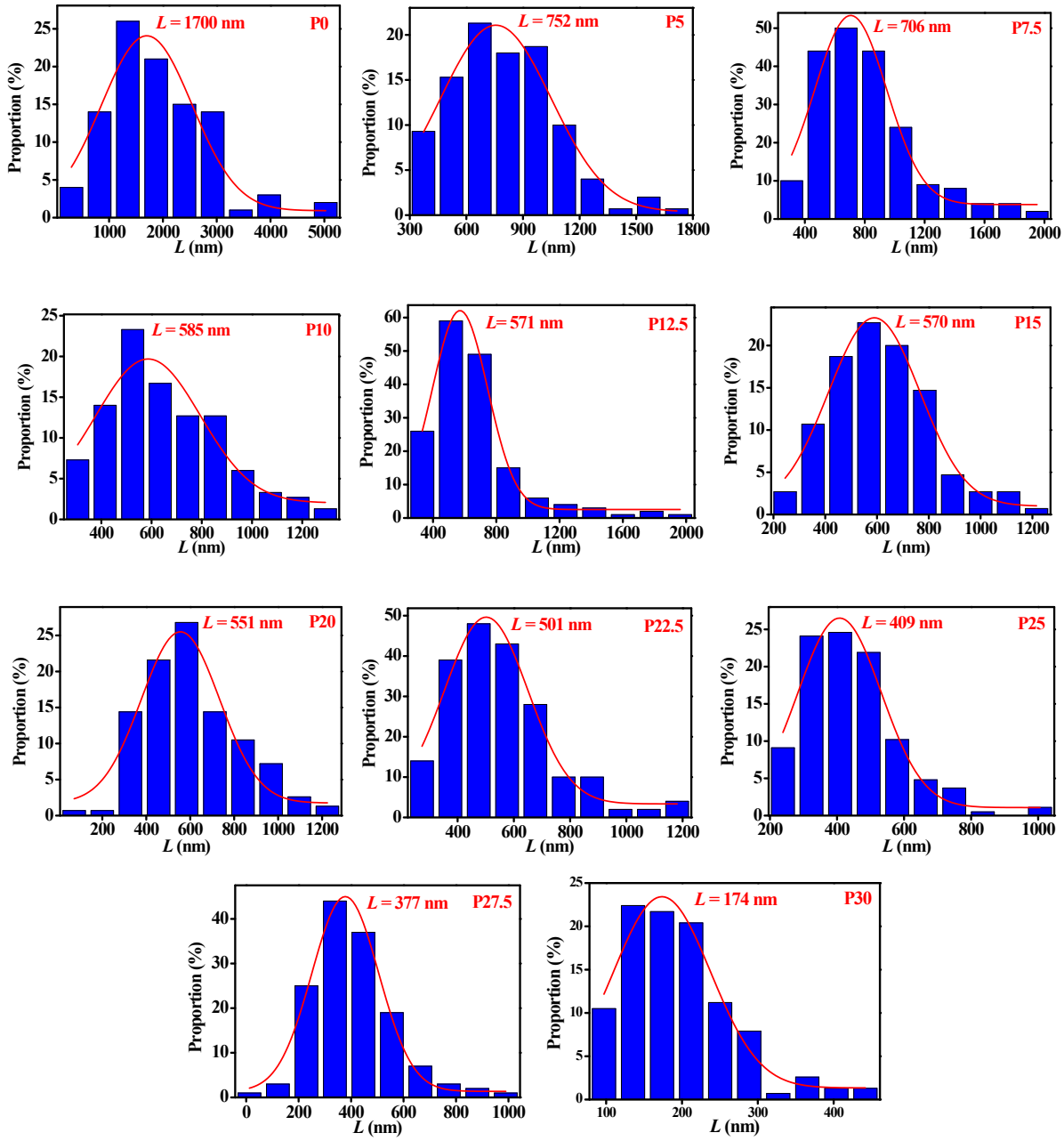

Fig. S2. Determination of lateral size (*L*) of the BiOBr samples by statics of more than three hundred of nanosheets, respectively. The solid lines were obtained by fitting the data to a Gaussian model.

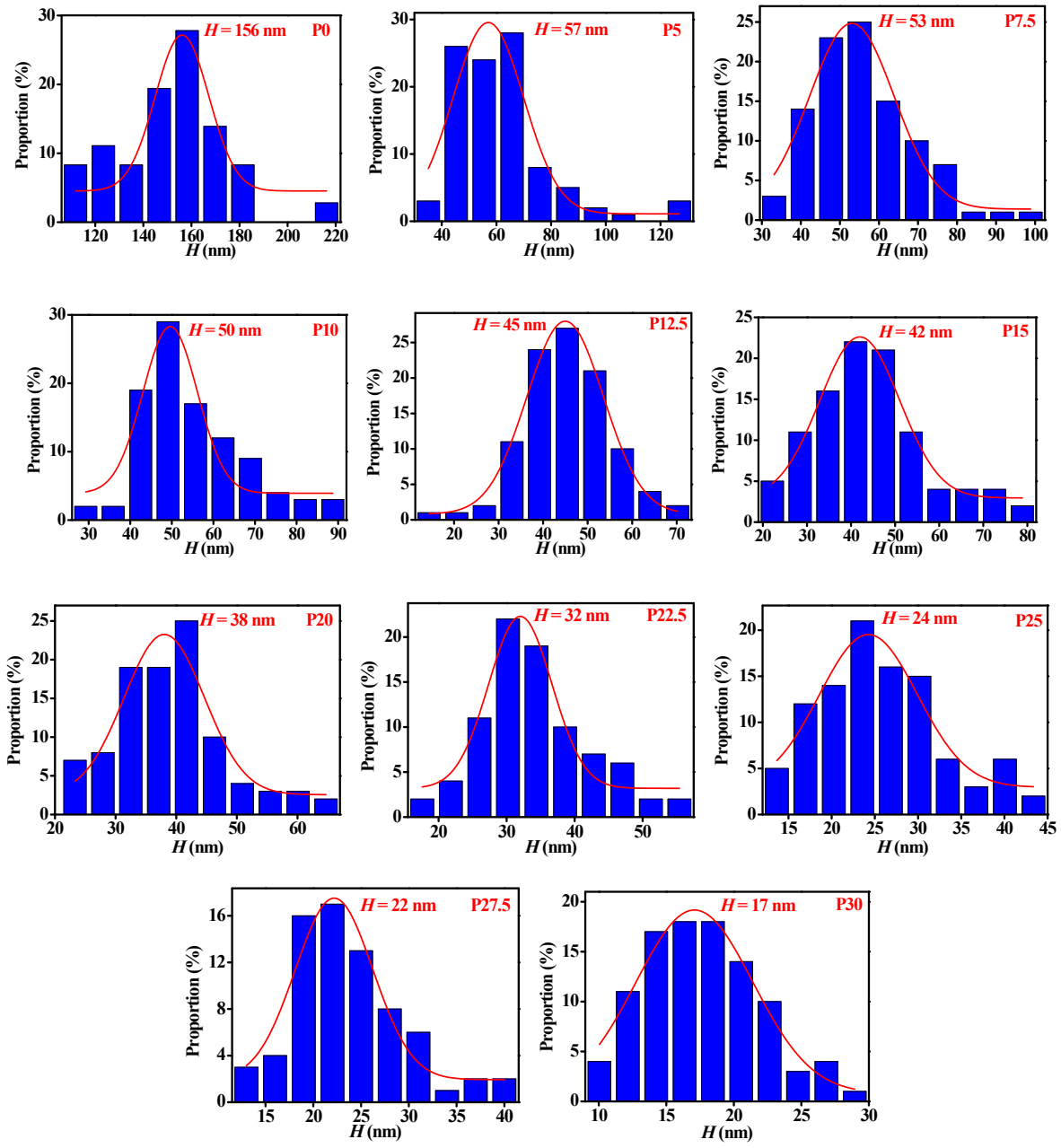

Fig. S3. Determination of average nanosheet thickness (*H*) of the BiOBr samples by statics of more than one hundred of nanosheets, respectively. The solid lines were obtained by fitting the data to a Gaussian model.

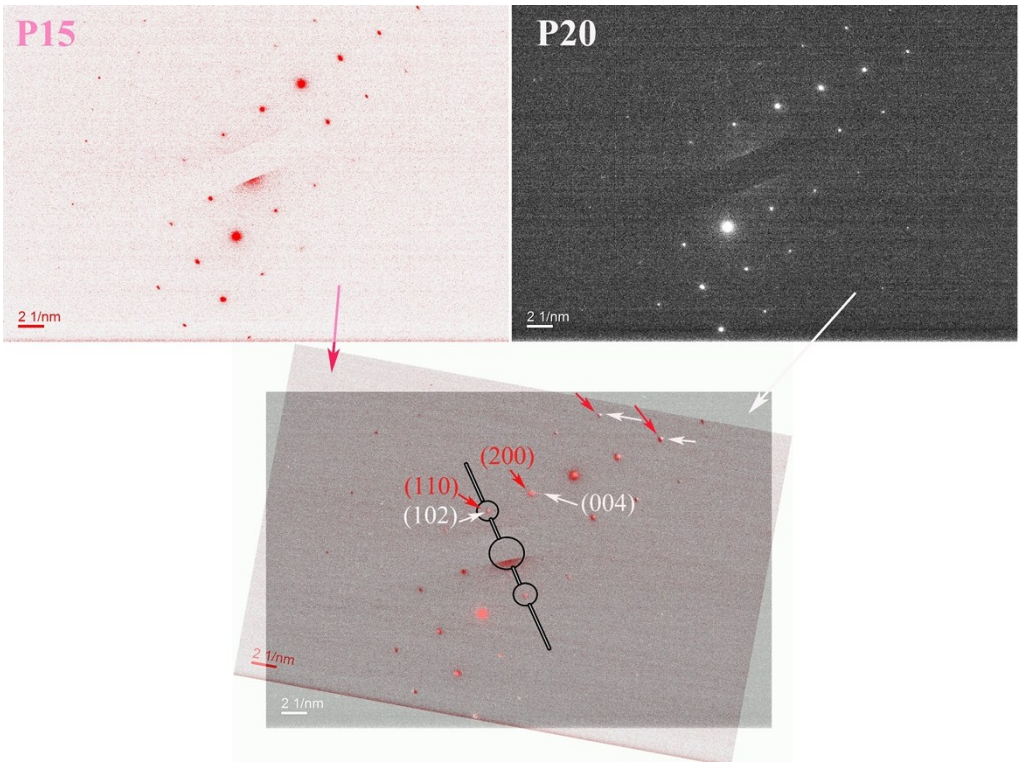

Fig. S4. SAED patterns of P15 (red spots), P20 (white spots) and superimposition of two patterns.

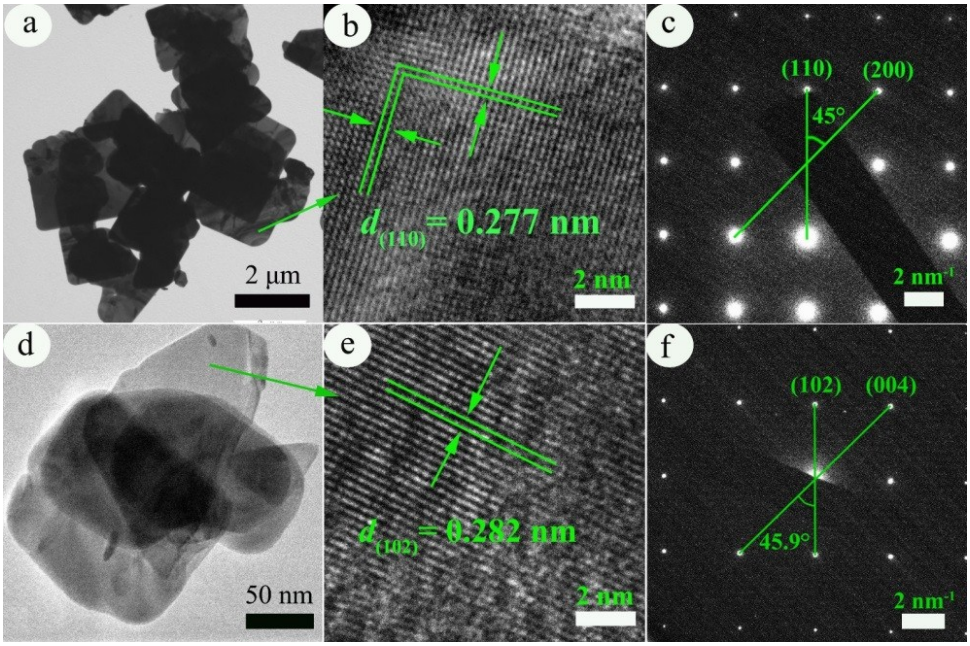

Fig. S5. (a, d) TEM, (b, e) HRTEM and (c, f) SAED images of (a–c) P0 and (d–f) P30.

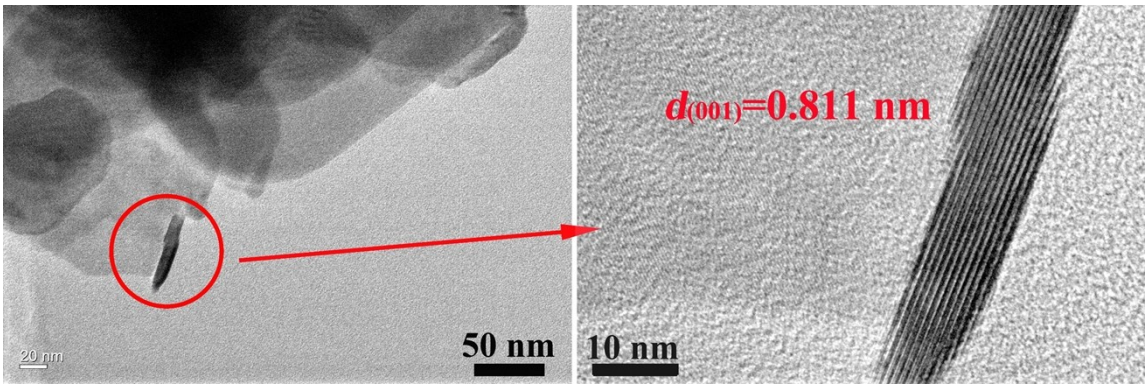

Fig. S6. HRTEM images of lateral side of P30.

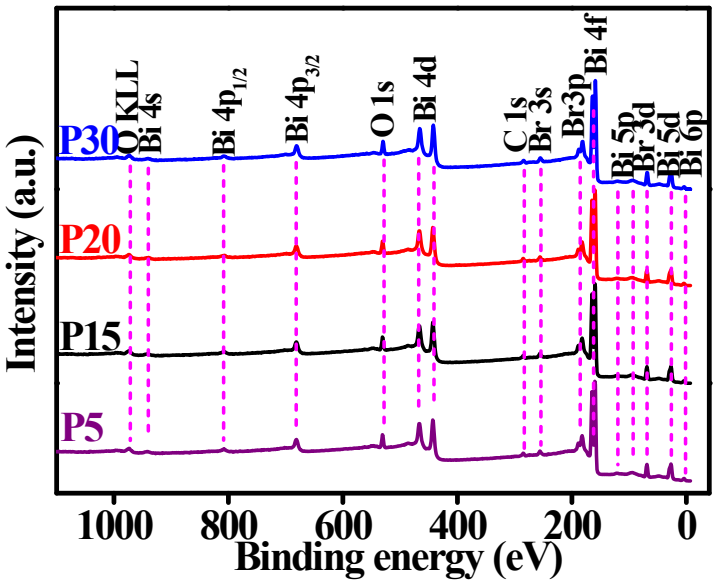

Fig. S7. XPS survey spectra of P5, P15, P20 and P30.

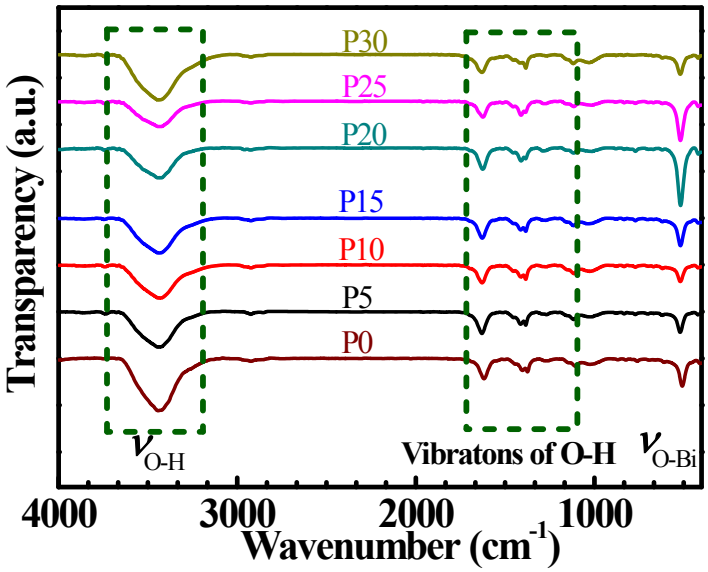

Fig. S8. FT-IR spectra of BiOCl samples.

There are no obvious absorption bands at 2800~3000 cm^{-1} which correspond to stretching vibration of $-CH_2$ and $-CH_3$,[1,2] indicating no organic compounds remain on the surfaces of BiOBr samples after filtration and washing. All the absorption bands in the figure are attributed to vibrations of O-H (surficial hydroxyl and adsorbed water) and O-Bi.[3–5]

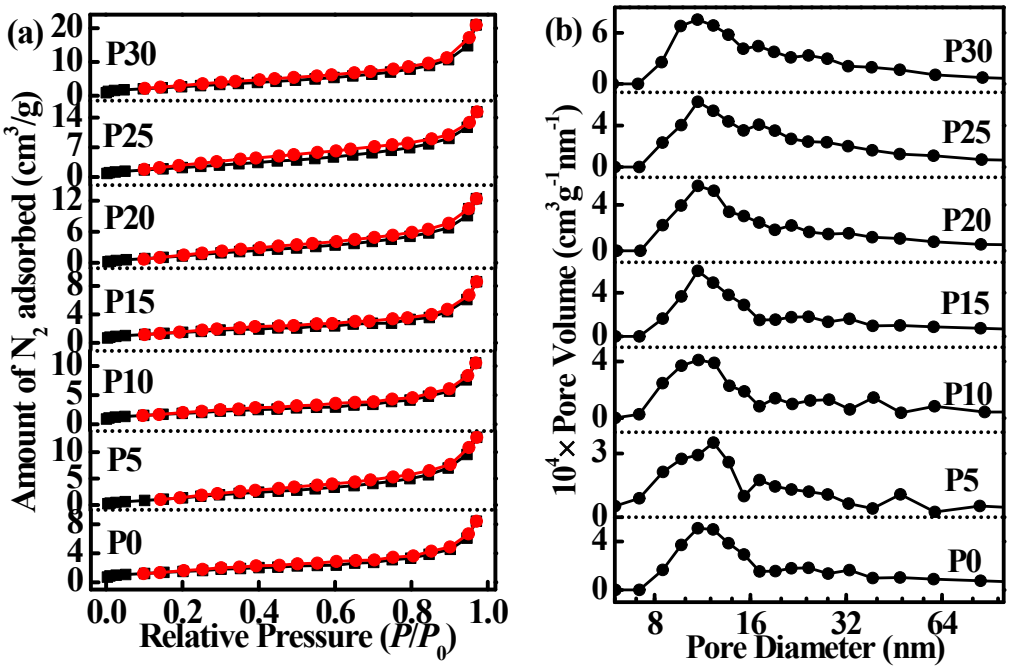

Fig. S9. (a) N_2 sorption isothermal and (b) pore size distribution curves of BiOBr nanosheets.

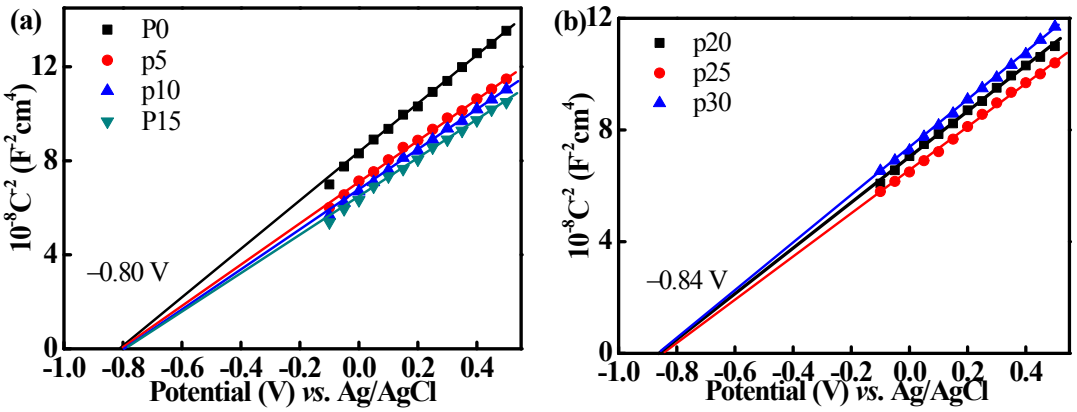

Fig. S10. Mott-Schottky plots of (a) P0–P15 and (b) P20–P30.

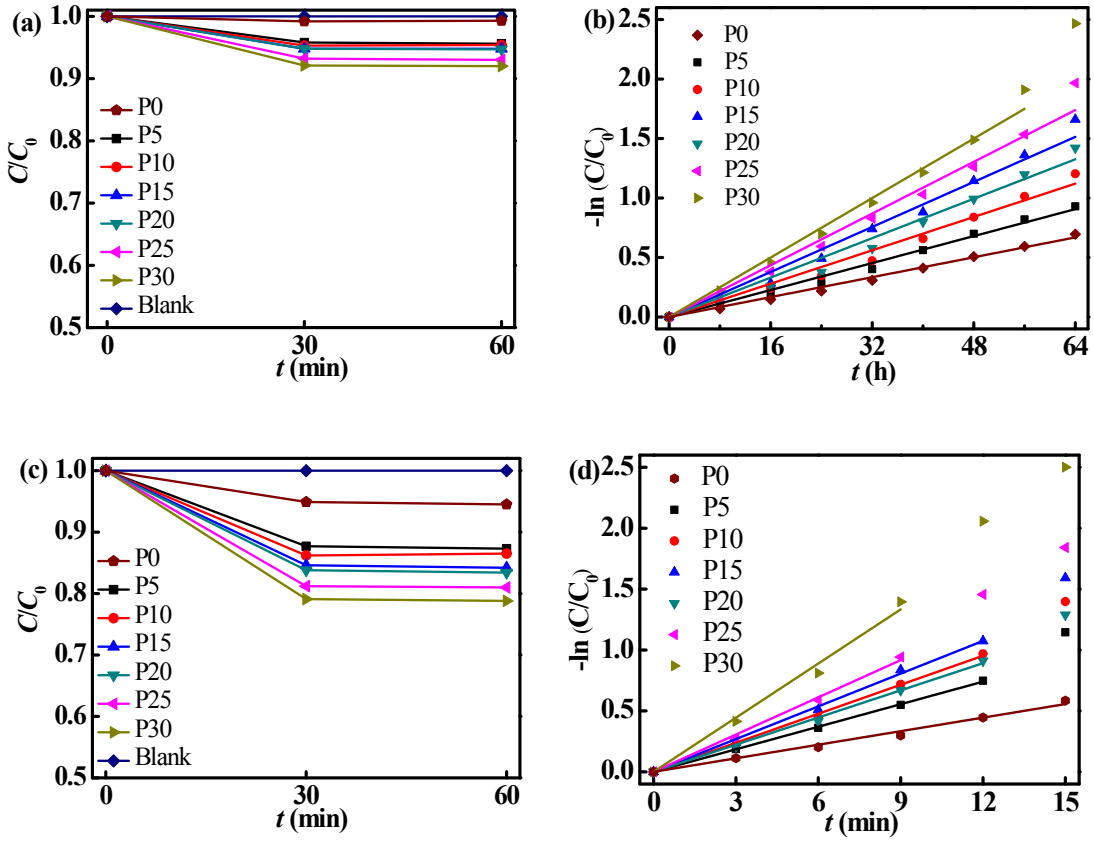

Fig. S11. (a, c) Adsorption of (a) SA and (c) (RhB) on photocatalysts and fitting plots of photodegradation data using the pseudo-first order kinetics model for (b) SA and (d) RhB.

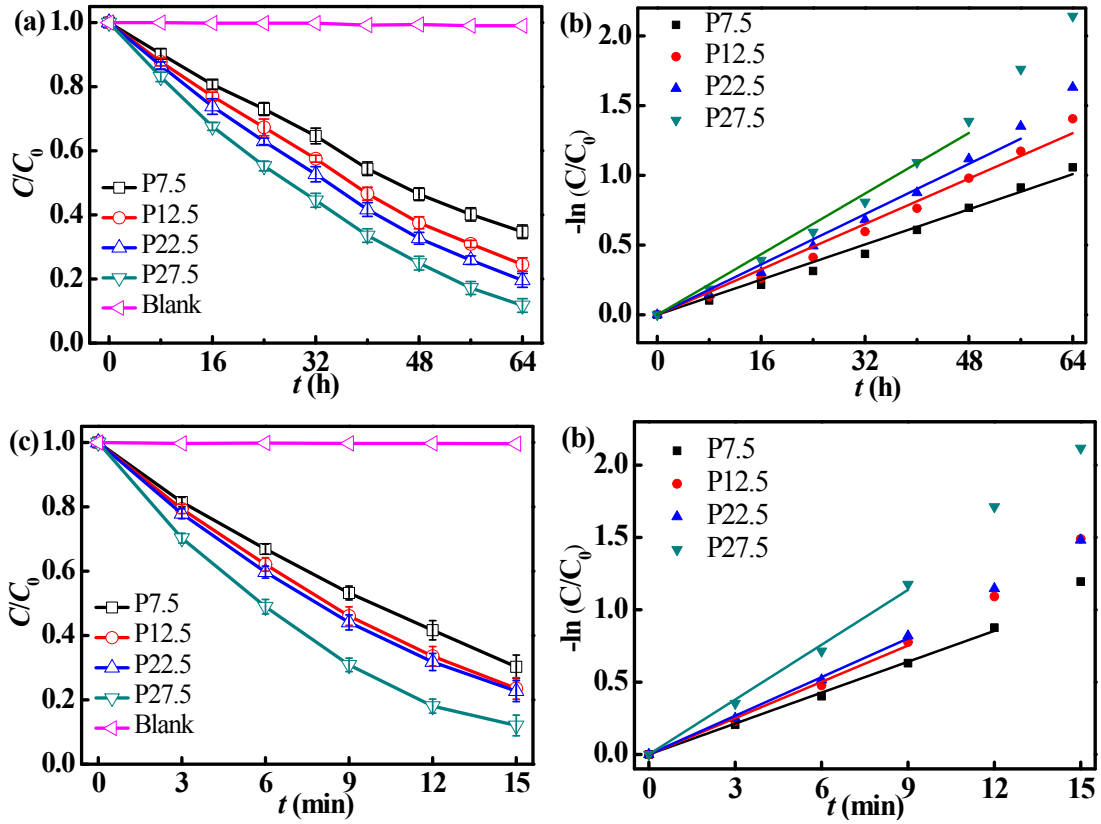

Fig. S12. (a, c) Photocatalytic degradation of (a) SA and (c) (RhB) on photocatalysts and (b, d) fitting plots of photodegradation data using the pseudo-first order kinetics model of (b) SA and (d) RhB on various photocatalysts.

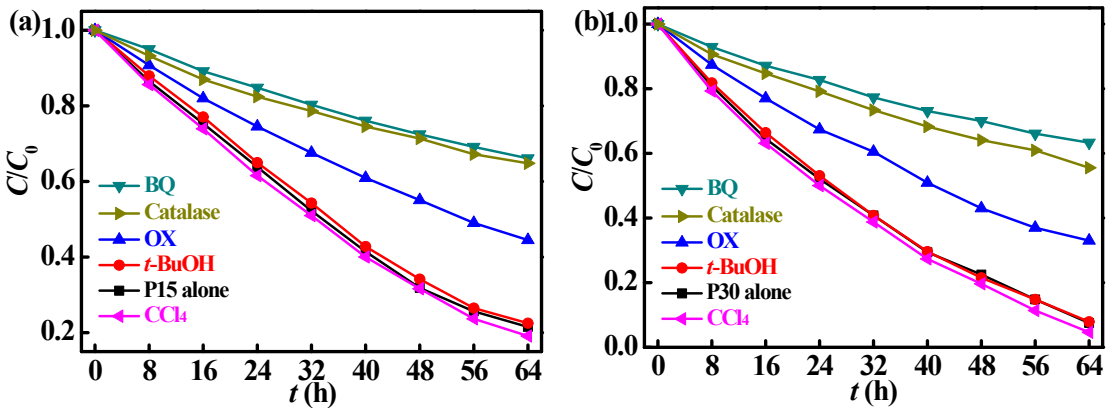

Fig. S13. Photocatalytic degradation of SA on (a) P15 and (b) P30 with different scavengers: BQ, 0.2 mM; OX, 0.4 mM; catalase 1×10^5 unit/L; *t*-BuOH, 40 mM; CCl_4, 5.2 mM.

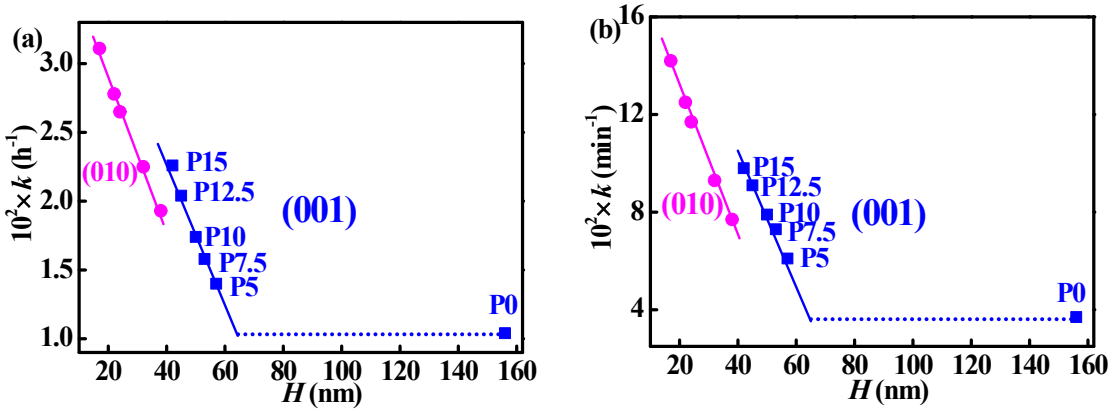

Fig. S14. Variation of pseudo-first-order kinetics rate constant (k) with average nanosheet thickness (H) of the samples for (a) SA and (b) RhB.

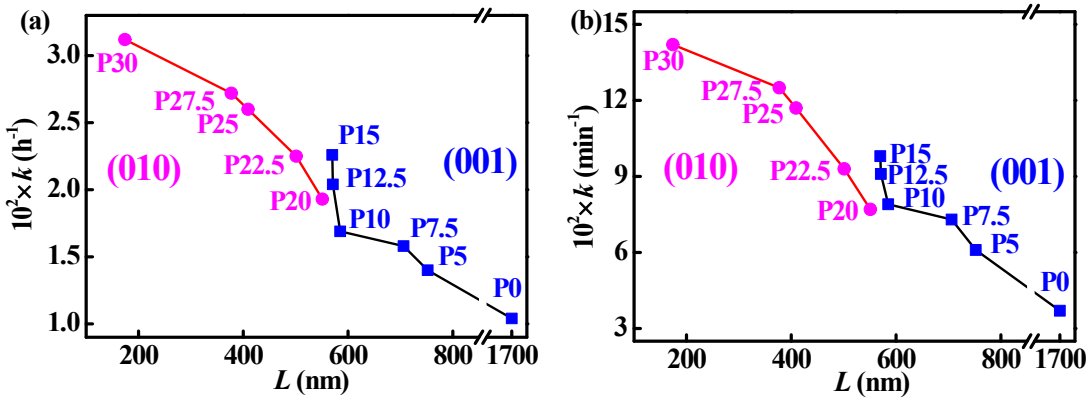

Fig. S15. Variation of pseudo-first-order kinetics rate constant (k) with average nanosheet length (L) of the samples for (a) SA and (b) RhB.

References

[1] Z. Liu, H. Ran, J. Niu, P. Feng, Y. Zhu, *J. Colloid Interface Sci.*, 2014, **431**, 187–193.

[2] G. Gupta, A. Kaur, A.S.K. Sinha, S.K. Kansal, *Mater. Res. Bull.*, 2017, **88**, 148–155.

[3] J. Xia, J. Di, S. Yin, H. Li, L. Xu, Y. Xu, C. Zhang, H. Shu, *Ceram. Int.*, 2014, **40**, 4607–4616.

[4] T.-X. Tao, J.-S. Dai, R.-C. Yang, J.-B. Xu, W. Chu, Z.-C. Wu, *Mater. Sci. Semicond.*

Process., 2015, **40**, 344–350.

[5] J. Di, J. Xia, M. Ji, B. Wang, S. Yin, Q. Zhang, Z. Chen, H. Li, *Appl. Catal.*, *B*, 2016, **183** 254–262.